Progress In Electromagnetics Research B, Vol. 101, 1–16, 2023

Defected Ground Structure Based High Gain, Wideband and High Diversity Performance Quad-Element MIMO Antenna Array for 5G Millimeter-Wave Communication

Ashok Kumar[1], Ashok Kumar[2, *], and Arjun Kumar[1]

Abstract—In this article, a planar compact grounded coplanar waveguide (GCPW)-fed 4-element multiple-input multiple-output (MIMO) antenna array with a defected ground structure (DGS) is demonstrated for the fifth generation (5G) millimeter-wave (mmWave) communication. Each element of the GCPW-fed mmWave MIMO antenna array contains a deformed pentagon-shaped radiating patch etched with a pair of identical circular slots in top surface and a DGS in bottom surface. To maintain low design complexity and compactness, a DGS is introduced and formed by embedding dual asymmetrical inverted T-shaped slots in the partial ground plane which enhance the gain and bandwidth of the antenna. The equivalent circuit model of the proposed DGS loaded GCPW-fed antenna is realized and presented. The proposed 4-element mmWave MIMO antenna array is realized by arranging the 4 identical antenna elements horizontally in a row with a distinct gap without any decoupling structure. It has the size of $1.02\lambda \times 3.86\lambda \times 0.021\lambda$ (at 25.66 GHz) and exhibits the measured bandwidth of 49.62% (25.30–42.0 GHz) with a peak gain of 12.02 dBi. Furthermore, the envelope correlation coefficient (ECC) < 0.0014, isolation > 24 dB between antenna elements, and channel capacity loss (CCL) < 0.29 bits/sec/Hz of the mmWave MIMO antenna array are attained over the entire mmWave frequency band.

1. INTRODUCTION

With the rapidly growing data traffic of the fifth generation (5G) wireless communication system, the mmWave technology has attracted much attention in industrial and academic applications such as 5G enabled portable devices, base stations, and internet of things (IoT) due to its potentiality of ultra-high data rate and large channel capacity [1, 2]. However, the associated high path loss attenuation, multi-path interference, and atmospheric absorption have limited the application of mmWave. Therefore, MIMO technique is introduced to increase the spectrum efficiency and coverage of mmWave wireless communication [3–6].

In the past years, great efforts have been made to design MIMO antennas for 5G enabled portable devices and base stations. Numerous MIMO antenna designs based on electronic band gap (EBG) [7, 8], DGS [9, 10], artificial magnetic conductor (AMC) [11, 12], dielectric resonator (DR) [13], loop and slot techniques [14–16], and substrate integrated waveguide (SIW) [17] have been proposed and can cover sub-6 GHz and mmWave bands. Aforementioned MIMO antenna designs suffer from the size, bandwidth, gain, isolation, and diversity problems. In this connection, a popular DGS technique can be utilized to improve the performance of the MIMO antenna designs. Moreover, numerous MIMO antenna designs based on DGS techniques [18–32] have been proposed for mmWave bands. Mostly

Received 6 March 2023, Accepted 14 June 2023, Scheduled 26 June 2023

* Corresponding author: Ashok Kumar (kumarashoksaini@gmail.com).

[1] School of Engineering and Applied Sciences, Bennett University, Greater Noida 201310, Uttar Pradesh, India. [2] Department of Electronics and Communication Engineering, Government Mahila Engineering College, Ajmer 305002, Rajasthan, India.

mmWave MIMO antenna designs have been compromised to some extent in size of antenna, planarity, bandwidth, gain, and diversity performance. By keeping these intended parameters and maintaining the antenna size along with planarity of the MIMO designs, the DGS technique will be further explored to accomplish wideband operation, high gain and isolation, and good diversity performance at mmWave bands.

In this article, a planar compact size DGS loaded 4-element MIMO antenna array is presented for 5G mmWave communication. Initially, the DGS loaded GCPW-fed mmWave antenna is connected by implementing a deformed pentagon-shaped radiating patch on the top surface and a DGS on the back surface to achieve wide bandwidth of about 47.72% (25.66–41.74 GHz). Further, a proposed DGS loaded 4-element mmWave MIMO antenna array is realized by arranging the 4 identical antenna elements horizontally in 1×4 manner (linearly in a row) with a distinct gap to achieve high isolation and high diversity performance without any decoupling structure between antenna elements. Finally, the proposed DGS based mmWave MIMO antenna array prototype is fabricated for demonstration, and performance is compared with the state-of-art mmWave MIMO antenna designs. The outcome of the proposed MIMO design is as follows:

- In comparison to cited state-of-art quad-element mmWave MIMO antenna designs, the proposed DGS based mmWave MIMO antenna array configuration has the smallest electrical size of $1.02\lambda \times 3.86\lambda \times 0.021\lambda$ and provides the widest bandwidth of about 49.62% (25.30–42 GHz), high isolation $>$ 24 dB, high gain of about 12.02 dBi, and high diversity performance especially ECC < 0.0014 and CCL < 0.29 bits/sec/Hz over the entire mmWave band which satisfy the requirement of mmWave systems.
- It is a planar design due to the simple structure of DGS and microstrip feed line, which make it easy to fabricate and integration in mmWave systems.
- It is a favourable candidate for future mmWave communication especially 5G enabled portable devices and base stations operating at n257 band (26.5–29.5 GHz), n260 band (37.0–40.0 GHz), n261 band (27.5–28.35 GHz), and other frequency range 2 (FR2) based future 5G new radio (NR) bands.

The entire paper is structured as follows. Section 2 elaborates the design and study of a single element mmWave antenna loaded with DGS. Sections 3 and 4 present the configuration and parametric study of a 4-element GCPW-fed mmWave MIMO antenna array, respectively. The measured results and diversity performance of 4-element DGS loaded mmWave MIMO antenna array are presented in Section 5. Section 6 concludes the outcomes of the presented study.

2. DESIGN AND ANALYSIS OF PROPOSED DGS LOADED MILLIMETER-WAVE ANTENNA

The schematic of the proposed single-element GCPW-fed mmWave antenna with DGS top and bottom views along with axis is shown in Figs. 1(a) and (b), respectively. The proposed mmWave antenna is composed of a deformed pentagonal shaped radiating element fed through 50 Ω GCPW feeding method

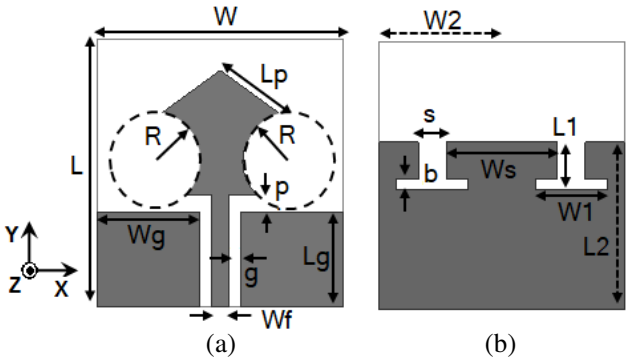

Figure 1. Schematic of proposed DGS loaded mmWave antenna: (a) top view, (b) bottom view.

having width W_f and gap g between them at top surface and DGS at bottom surface of the antenna. The deformed pentagon-shaped radiating element is formed by etching a pair of symmetrical circular slots of radius R in pentagonal patch, and DGS is formed by loading a pair of asymmetrical inverted T-shaped slots (arm length L_1 and arm width W_1) in the partial ground plane of length L_2. The asymmetrical inverted T-shaped slots are separated with width W_s. By introducing DGS in the deformed pentagon-shaped mmWave antenna, it alters the current distribution path which improves mainly the antenna gain and bandwidth at mmWave frequency range. It is printed on a Rogers RT/duroid 5880 substrate having the relative permittivity ε_r of 2.2, height of 0.254 mm (10 mil), and loss tangent $\tan\delta = 0.0009$ with the antenna dimension of $L \times W$. It has an overall size of $12 \times 11 \times 0.254\,\text{mm}^3$ which corresponds to $1.02\lambda \times 0.94\lambda \times 0.021\lambda$, where λ is the wavelength at 25.66 GHz (lowest frequency). The proposed DGS loaded mmWave antenna is simulated and optimized through EM simulation tool Ansys HFSS 21.1. The design parameters of the proposed DGS loaded mmWave antenna are outlined in Table 1.

Table 1. Parameters of the proposed DGS loaded single element mmWave antenna.

Parameters	L	W	Lg	Wg	Wf	g	p	R
Dimension (mm)	12	11	4.25	4.55	0.78	0.56	0.75	2
Parameters	Lp	s	b	$L1$	$W1$	$L2$	$W2$	Ws
Dimension (mm)	3.6	1.25	0.5	2.15	3.25	7.5	5.5	5

The four evolution steps of the proposed deformed pentagon-shaped mmWave antenna with DGS are illustrated in Fig. 2. In Step-1, a conventional GCPW-fed pentagon-shaped antenna with ground plane (Ant. 1) is designed as shown in Fig. 2(a). It is observed that the surface current of Ant. 1 is mainly concentrated on the pentagonal patch of GCPW-fed antenna which creates the resonance at about 36.85 GHz and provides the narrow bandwidth of about 3.64%. In Step-2, by introducing a pair of symmetrical circular slots having radius R in the pentagonal patch (Ant. 2) as presented in Fig. 2(b), it will create the additional resonance at about 41.15 GHz. Both resonances at about 35.85 GHz and 41.15 GHz are created due to the concentration of surface current mainly on the deformed pentagonal patch and the arcs of circular slots in analogous orientation of GCPW-fed antenna, respectively. For

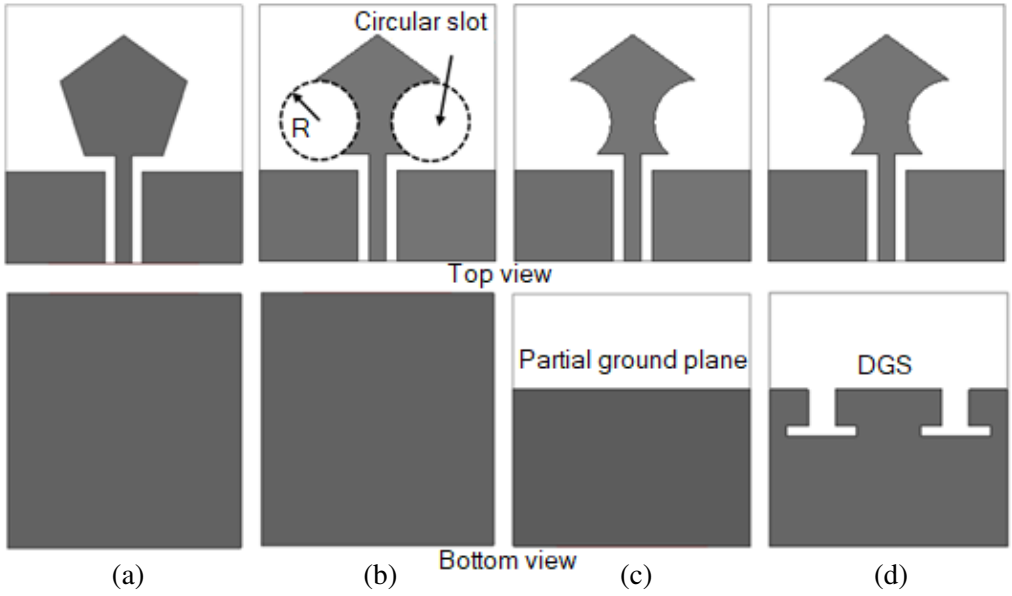

Figure 2. Evolution process of the proposed DGS loaded mmWave antenna: (a) Ant. 1, (b) Ant. 2, (c) Ant. 3, and (d) Ant. 4.

instance, when circular slots of radius $R = 1$ mm are considered, additional weak resonance at about 42 GHz is observed. Further, when the radius R of circular slots is increased from 1 mm to 2 mm, the additional resonance is shifted from 42 GHz to 41.15 GHz which is due to lengthening the surface current path on the arcs of circular slots. Both resonances exhibit narrow bandwidths. As we know, the concept of partial ground plane is a well-known technique to accomplish wideband characteristics. Therefore, in Step-3, a partial ground plane of length L_2 is introduced in Ant. 2 (Ant. 3 of Fig. 2), and the dual resonance bands created in Step 2 are merged effectively into a broader one. It provides a wide frequency span (f_{span}) of about 10.26 GHz and wideband response along with improvement in gain of the antenna. In Step 4, two asymmetrical inverted T-shaped slots are embedded in the bottom ground of Ant. 3 (Ant. 4 of Fig. 2) as DGS to modify the ground current distribution which offer a wide frequency span about 16.08 GHz and peak gain about 5.41 dBi.

To construct the equivalent circuit model of Ant. 4, the proposed DGS loaded mmWave antenna is divided into three steps (i.e., CPW feed, patch, and DGS), and an equivalent circuit of entire structure is shown in Fig. 3. For validation of the antenna structure, an equivalent circuit is built, tuned, and optimised in AWRMicrowave Office ver. 22.1, and component values are mentioned in Fig. 3. The $|S_{11}|$ computed by using equivalent circuit for Ant. 4 (proposed antenna) is shown in Fig. 4(a). The $|S_{11}|$ and gain for Ant. 1–Ant. 4 are shown in Figs. 4(a) and (b), respectively, and summarized in Table 2.

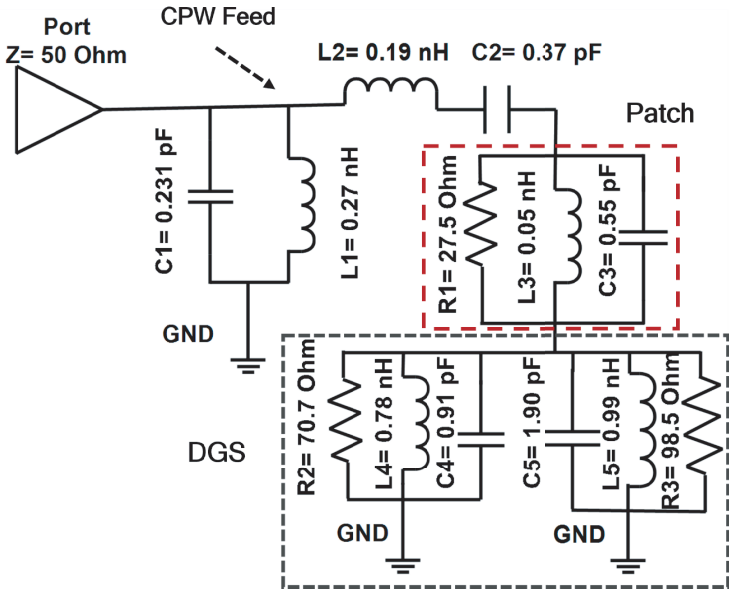

Figure 3. Equivalent circuit diagram of the proposed DGS loaded mmWave antenna.

Table 2. Summary of impedance bandwidth (IBW) and gain of Ant. 1–Ant. 4.

S. No.	Antenna Configurations	IBW (GHz, $f_{span\|\,GHz}$,$f_{c\|\,GHz}$, %)	Gain variation (dBi)
1.	Ant. 1	35.92–37.24, 1.32, 36.23, 3.64	2.79–3.02
2.	Ant. 2	35.38–36.32, 0.94, 35.85, 2.62 40.62–41.38, 0.76, 41.00, 1.85	3.11–3.26 2.16-2.18
3.	Ant. 3	30.74–41.00, 10.26, 35.87, 28.60	3.50–4.02
4.	Ant. 4	25.66–41.74, 16.08, 33.70, 47.72	3.60–5.41

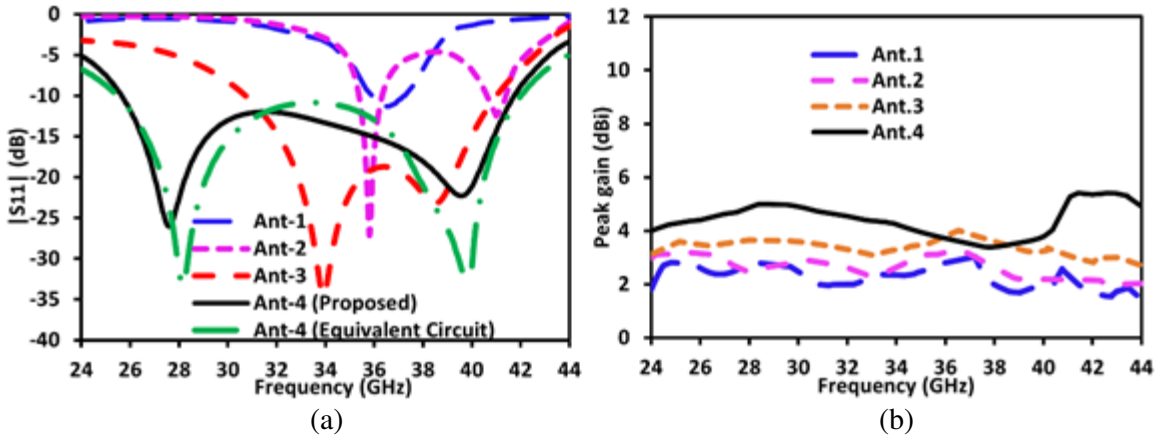

Figure 4. Simulated results of Ant. 1–Ant. 4 configurations: (a) $|S_{11}|$ plot, (b) peak gain plot.

3. DESIGN AND ANALYSIS OF PROPOSED DGS LOADED FOUR-ELEMENT MMWAVE MIMO ANTENNA ARRAY

Based on the single element mmWave antenna discussed in Section 2, the top and bottom views of 4-element DGS loaded mmWave MIMO antenna array configuration are presented in Figs. 5(a) and (b), respectively. Based on the conventional array design methodology, it is realized by using 4 identical elements that would be placed symmetrically in a 1×4 manner (linearly in a row) with a distinct gap of $d = 0.4\,\text{mm}$ (0.03λ) between individual antenna elements on a single substrate (RT/duroid 5880) having thickness 10 mil, $\varepsilon_r = 2.2$ and $\tan\delta = 0.0009$, which has an overall MIMO antenna dimension of $L_m \times W_m$ $(12 \times 45.2\,\text{mm}^2$ which corresponds to $1.02\lambda \times 3.86\lambda$ at 25.66 GHz). Such a placement approach creates a gap between individual antenna elements which increases the spacing between adjacent antenna radiating elements, thus the isolation of the proposed MIMO array configuration is improved. In this configuration, the top and bottom ground of nearby antennas do not overlap, and wideband response of the DGS loaded MIMO antenna remains unaffected as compared to single-element antenna with DGS,

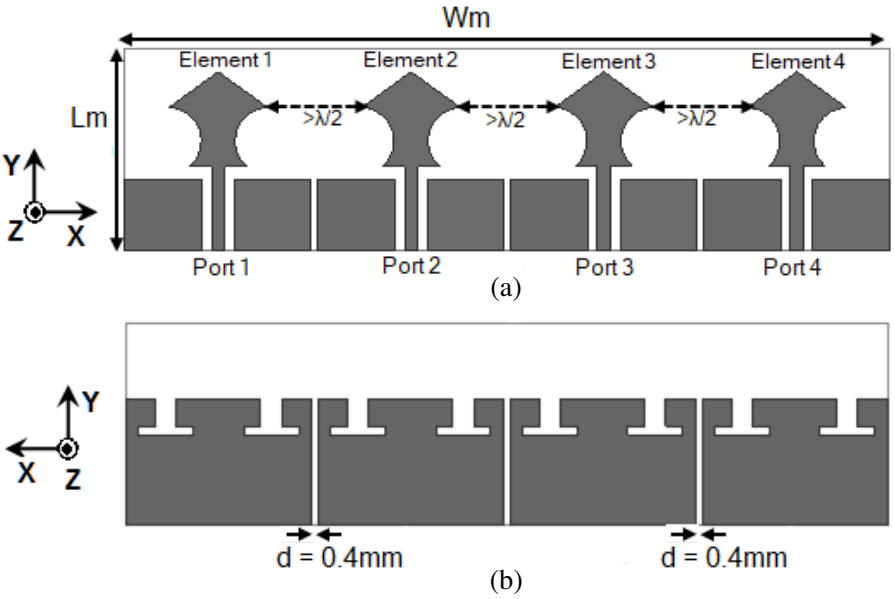

Figure 5. Layout of proposed 4-element DGS based mmWave MIMO antenna array: (a) top view, (b) bottom view.

which has 24.86–41.48 GHz (simulated by using HFSS 21.1). For good isolation, the minimum spacing of 5.61 mm ($0.48\lambda \approx \lambda/2$) is between the centers of deformed pentagonal shaped radiating elements, and no decoupling technique is considered. From MIMO antenna prospective, the decoupling mechanism is a technique that relies on embedding additional structure to counteract the mutual coupling or to improve the isolation between antenna elements. For excellent isolation, the radiating elements spacing should be less than one wavelength ($< \lambda$). The reason for considering 1×4 MIMO antenna configuration is to enhance the radiation characteristics and diversity performance. The transmission coefficient parameters of the proposed DGS based 4-element mmWave MIMO antenna array are shown in Fig. 6(a). It can be perceived that the isolation between two adjacent elements 1–2, 2–3, 3–4 ($|S_{12}| = |S_{21}|$, $|S_{23}| = |S_{32}|$, $|S_{34}| = |S_{43}|$) is identical over operating bandwidth and about > 24 dB, as transmission coefficient is below -24 dB. Correspondingly, the isolation between antenna elements 1–3 and 2–4 ($|S_{13}| = |S_{31}|$, $|S_{24}| = |S_{42}|$) is identical over bandwidth and about > 33 dB, as transmission coefficient is below -33 dB. Similarly, the isolation between antenna elements 1 and 4 ($|S_{14}| = |S_{41}|$) is about > 42 dB, as transmission coefficient is below -42 dB. From the analysis, it is concluded that minimum isolation between antenna elements 1 and 2 is 24 dB perceived which confirms the high performance of the proposed DGS loaded mmWave MIMO antenna array.

In order to understand the impact of gap d, the simulated S-parameters are depicted in Fig. 6(b). When the distinct gap $d = 0$ mm, it means the ground plane is fully connected, and the proposed design works as a MIMO antenna. Conversely, if the gap $d > 0$ mm is considered, then the proposed design works as a MIMO antenna array. It can be seen from Fig. 6(b) that wideband responses of the proposed design in both cases remain unaffected, but the minimum isolation about 3 dB is improved when distinct gap $d = 4$ mm (0.03λ) is utilized. So, the proposed design works as a MIMO antenna array which is realized by placing all 4 identical antenna elements with a distinct gap of $d = 4$ mm (0.03λ) on a single substrate to improve the isolation between antenna elements.

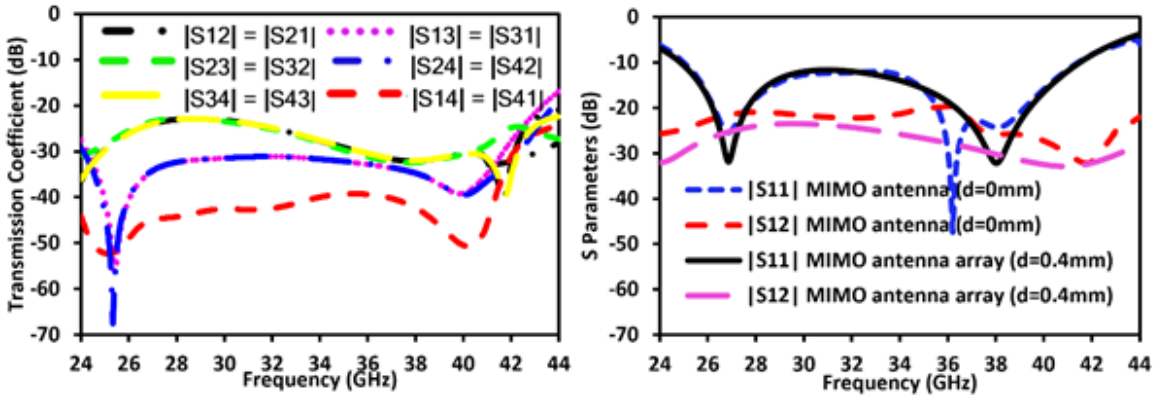

(a) (b)

Figure 6. Simulated results of the proposed DGS based 4-element mmWave MIMO antenna array: (a) transmission coefficient parameters, (b) variation in gap d on S-parameters.

Further, to realize the effects related with the excitation of DGS based single-element antenna on the adjacent antenna elements, the magnitude of current density at 27 GHz resonance is depicted in Fig. 7. When antenna element 1 (port 1) of MIMO antenna is excited, and remaining antenna elements 2, 3, and 4 (ports 2, 3 and 4) are matched with 50 Ω load, the magnitude of current density is mainly observed on the excited antenna element as depicted in Fig. 7(a). Correspondingly, when antenna elements 2/3/4 (ports 2/3/4) are excited, and remaining elements are matched through 50 Ω load, the magnitude of current density is mainly observed on the excited antenna element as demonstrated in Figs. 7(b) to (d), respectively. From the study, it is concluded that the excited antenna element has slight impact on adjacent antenna elements which slightly deteriorates isolation but does not affect the remaining antenna elements which leads to offering high isolation and low mutual coupling between elements.

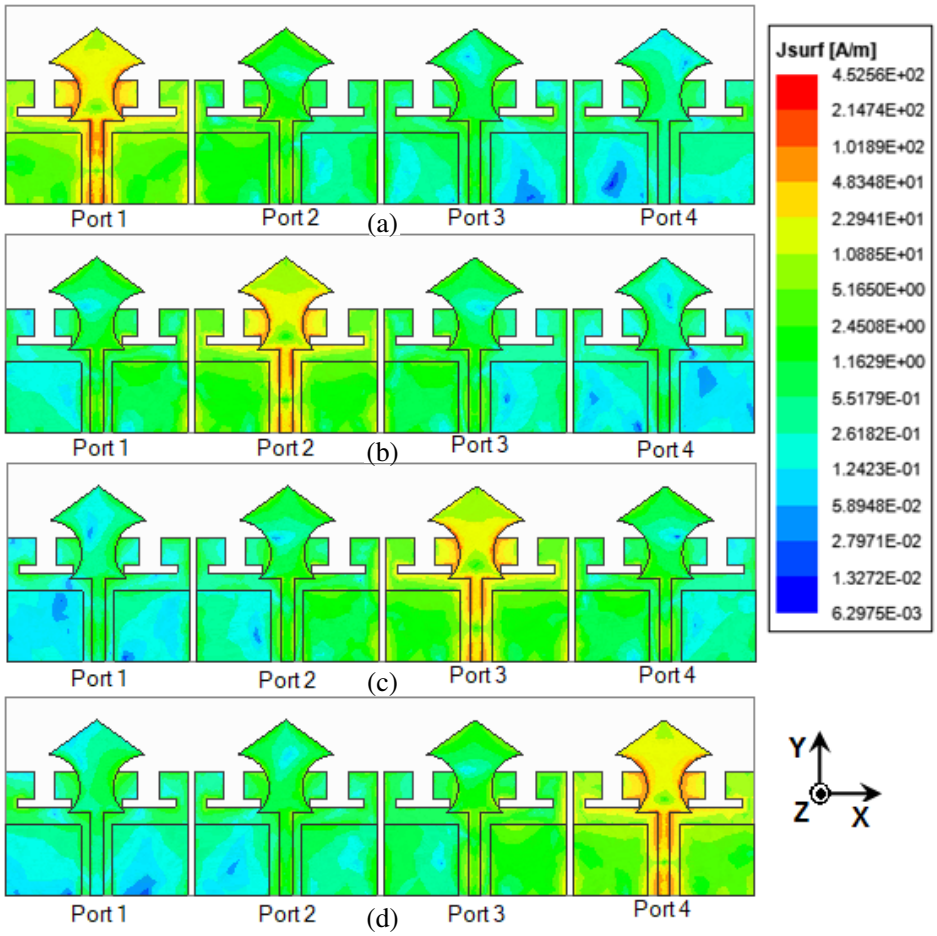

Figure 7. Magnitude of current density of DGS based 4-element mmWave MIMO antenna array at 27 GHz when (a) port-1 excited, (b) port-2 excited, (c) port-3 excited, (d) port-4 excited.

4. PARAMETRIC STUDY

The impact of an asymmetrical inverted T-shaped slot DGS with width s and length L_1 on S-parameters of the proposed DGS loaded 4-element mmWave MIMO antenna array is presented in this section. Now, the variation in slot width s and length L_1 of DGS is investigated on S-parameters ($|S_{11}|$ and $|S_{21}|$) and presented when antenna element 1 (port 1) is excited, and remaining antenna elements 2, 3, and 4 (ports 2, 3 and 4) are matched through 50 Ω load.

4.1. Impact of Asymmetrical Inverted T-Shaped Slot DGS Width s

Figure 8 depicts the impact of an asymmetrical inverted T-shaped slot DGS width s on S-parameters ($|S_{11}|$ and $|S_{21}|$) of the proposed DGS loaded 4-element mm-Wave MIMO antenna array when s varies from 1.21 mm to 1.29 mm. At s = 1.21 mm and 1.23 mm, the MIMO antenna with DGS provides dual-band response with isolation > 20 dB whereas increasing s from 1.25 mm to 1.29 mm, it exhibits wideband response along with isolation > 24 dB between adjacent elements. It is also perceived that with the transition of s value from 1.23 mm to 1.25 mm, the dual resonance bands are merged effectively into a broader one and exhibit wideband behaviour. Based on the study, the optimum value of s = 1.25 mm is taken for the widest bandwidth about 50.10% (frequency span, f_{span} = 16.62 GHz). The impact of DGS slot width s on IBW and isolation is summarized in Table 3.

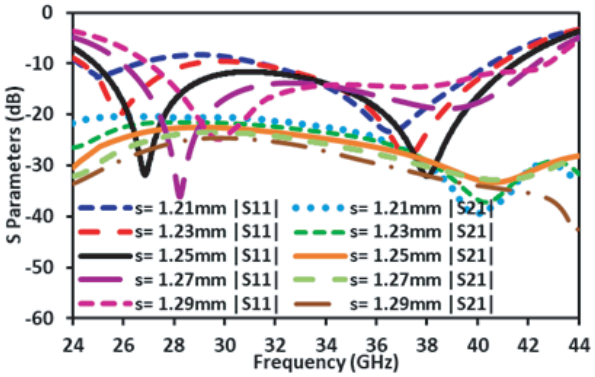

Figure 8. Impact of asymmetrical inverted T-shaped slot DGS width s on S-parameters.

Table 3. Summary of IBW and isolation by varying DGS slot width s.

S. No.	Varying parameter	IBWs (GHz, $f_{\text{span}\vert\,\text{GHz}}$, $f_{\text{c}\vert\,\text{GHz}}$, %)	Isolation (dB)
1.	$s = 1.21$ mm	24.26–26.58, 2.32, 25.42, 9.12 31.42–40.52, 9.10, 35.97, 25.29	> 20 > 22
2.	$s = 1.23$ mm	24.38–28.80, 4.42, 26.59, 16.62 31.06–40.88, 9.82, 35.97, 27.30	> 22 > 24
3.	**$s = 1.25$ mm**	**24.86–41.48, 16.62, 33.17, 50.10**	**> 24**
4.	$s = 1.27$ mm	25.96–42.30, 16.34, 34.13, 47.87	> 24
5.	$s = 1.29$ mm	27.0–42.74, 15.74, 34.87, 45.13	> 25

4.2. Impact of Asymmetrical Inverted T-Shaped Slot DGS Length L_1

The impact of the asymmetrical inverted T-shaped slot length L_1 on S-parameters ($|S_{11}|$ and $|S_{21}|$) when L_1 varies from 1.85 mm to 2.25 mm is depicted in Fig. 9. When the DGS length L_1 is increased from 1.85 mm to 2.15 mm, the operating band shifts towards lower side, and the overall bandwidth increases from 45.89% to 50.10%, but isolation (> 24 dB) is almost unaffected. At $L_1 = 2.25$ mm, the operating band shifts towards upper side, and the overall bandwidth along with isolation decreases. Based on the study, the best suited slot length value $L_1 = 2.15$ mm is chosen to get the widest bandwidth of about 50.10% ($f_{span} = 16.62$ GHz). The impact of DGS slot length L_1 on IBW and isolation is summarized in Table 4.

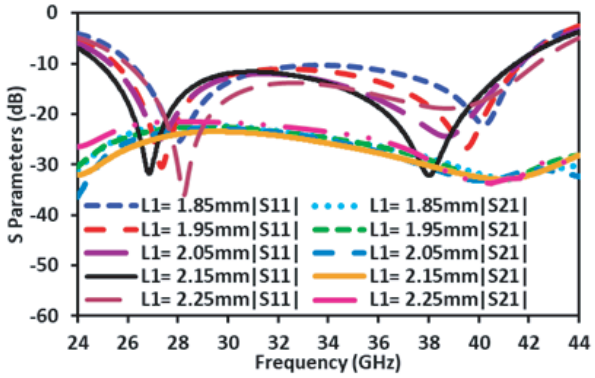

Figure 9. Impact of asymmetrical inverted T-shaped slot DGS length L_1 on S-parameters.

Table 4. Summary of IBW and isolation by varying DGS slot length L_1.

S. No.	Varying parameter	IBWs (GHz, $f_{\text{span}\mid\text{GHz}}$, $f_{\text{c}\mid\text{GHz}}$, %)	Isolation (dB)
1.	$L_1 = 1.85\,\text{mm}$	26.12–41.68, 15.56, 33.90, 45.89	> 24
2.	$L_1 = 1.95\,\text{mm}$	25.52–41.68, 16.16, 33.60, 48.09	> 24
3.	$L_1 = 2.05\,\text{mm}$	25.30–41.60, 16.30, 33.45, 48.72	> 24
4.	$L_1 =$**2.15 mm**	**24.86–41.48, 16.62, 33.17, 50.10**	> 24
5.	$L_1 = 2.25\,\text{mm}$	25.96–42.30, 16.34, 34.13, 47.87	> 22

5. RESULTS AND DISCUSSION

The results and diversity performance of the proposed DGS loaded 4-element mmWave MIMO antenna array are discussed in the section. It is simulated by using 3D EM simulator HFSS and CST Microwave Studio (MWS) software.

5.1. Results Analysis of DGS Based mmWave MIMO Antenna Array

To investigate and validate the performance of the proposed DGS based 4-element MIMO antenna array, the prototype MIMO antenna array is fabricated on a Rogers RT/duroid 5880 substrate with the size of $12 \times 45.2 \times 0.254\,\text{mm}^3$ ($1.02\lambda \times 3.86\lambda \times 0.021\lambda$, where λ is the wavelength at 25.66 GHz) as depicted in Fig. 10(a). To excite the proposed MIMO antenna, four K-type gold plated RF 50 Ω, air dielectric 2.92 mm coaxial SMA connectors are utilized carefully to feed the antenna. These 2.92 mm SMA connectors allow electrical performance to 40 GHz. The measurement setup photograph of an anechoic chamber is depicted in Fig. 10(b). The simulated $|S_{11}|$ and $|S_{21}|$ of the proposed DGS based MIMO antenna array by using EM simulator HFSS and CST MWS and measured through Agilent N5247A vector network analyzer (VNA) are compared and demonstrated in Fig. 10(c). The maximum simulated −10 dB bandwidths of proposed DGS based 4-element mmWave MIMO antenna array by using HFSS and CST MWS are 16.62 GHz (24.86–41.48 GHz) and 16.32 GHz (25.28–41.60 GHz), respectively, while the measured one is 16.70 GHz (25.30–42.00 GHz). The minimum $|S_{11}|$ is about −33 dB at 27.10 GHz and −33.25 dB at 38.0 GHz. It is also perceived from Fig. 10(c) that the minimum isolation between antenna elements 1 and 2 (port 1 and 2) is 24 dB. The slight deviation between results (measured and simulated) is due to misalignment/assembly of its parts, applied boundary conditions in simulation, and

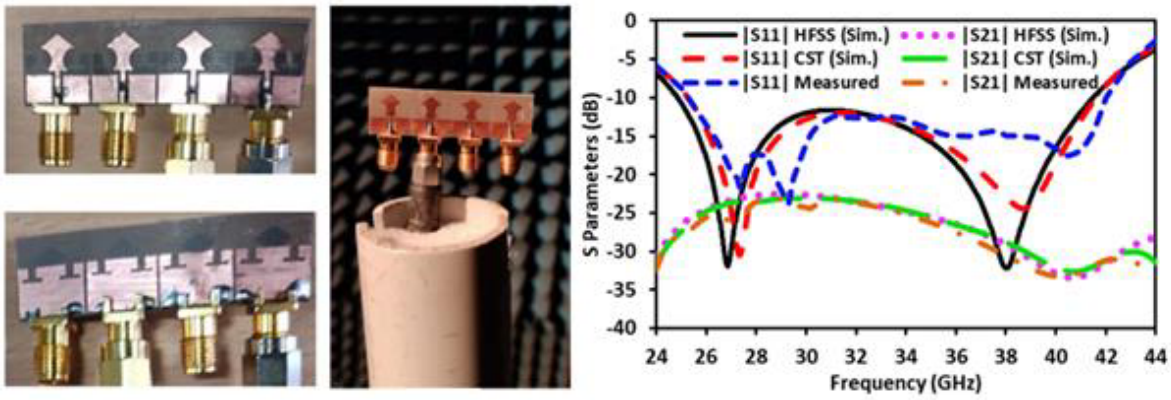

(a) (b) (c)

Figure 10. (a) Fabricated prototype of proposed DGS based mmWave MIMO antenna array, (b) measurement setup in anechoic chamber, (c) comparison of S-parameters.

fabrication errors.

The peak gain and radiation efficiency (η) of the proposed DGS based mmWave MIMO antenna array is depicted in Fig. 11. It can be perceived that the deformed pentagon-shaped single-element antenna with DGS provides the peak gain about 5.41 dBi whereas two-element DGS based mmWave MIMO antenna has the peak gain of 7.74 dBi which is about 30% higher than single-element antenna with DGS. Correspondingly, the simulated peak gains of the 4-element mmWave MIMO antenna array with DGS using HFSS and CST MWS are about 12.24 dBi and 12.18 dBi, respectively, whereas the measured peak gain is about 12.02 dBi. It can be perceived that the peak gain is enhanced about 55.8% and 36.8% of the 4-element mmWave MIMO antenna as compared to single-element mmWave antenna with DGS and 1×2 MIMO antenna configuration, respectively. The simulated η by using HFSS and CST MWS is more than 80% achieved over the entire mmWave band. The comparisons of simulated and measured -10 dB bandwidths, peak gains, and η are summarized in Table 5.

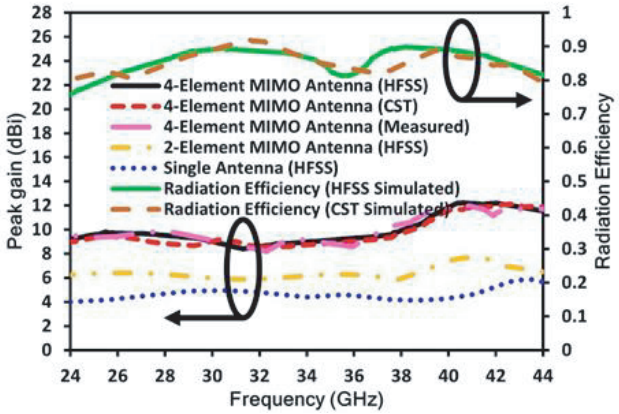

Figure 11. Peak gain and radiation efficiency of the proposed DGS based mmWave MIMO antenna array.

Table 5. Comparisons of simulated and measured -10 dB bandwidths, peak gains and efficiency of the proposed DGS based mmWave MIMO antenna array.

S. No.	Antenna Type	IBW (GHz, $f_{\text{span}\|\text{GHz}}$, $f_{\text{c}\|\text{GHz}}$, %)	Peak Gain (dBi)	η (%)
1.	Simple element antenna with DGS	25.66–41.74, 16.08, 33.70, 47.72	5.41	—
2	2-element MIMO antenna array with DGS	25.52–41.68, 16.16, 33.60, 48.09	7.74	—
2.	4-element MIMO antenna array with DGS (HFSS)	24.86–41.48, 16.62, 33.17, 50.10	12.24	> 80
3.	4-element MIMO antenna array with DGS (CST)	25.28–41.60, 16.32, 33.44, 48.80	12.18	> 82
4.	4-element MIMO antenna array with DGS (Measured)	25.30–42.00, 16.70, 33.65, 49.62	12.02	—

The normalized far-field radiation patterns (measured and simulated) of the proposed DGS based 4-element mmWave MIMO antenna array in two principal planes, i.e., XZ-plane ($\phi = 0°$) and YZ-plane ($\phi = 90°$) at 27 and 38 GHz resonance frequencies, are plotted in Figs. 12(a) and (b), respectively. The measured co-pol and cross-pol results are in good agreement with simulated ones through HFSS and CST MWS simulation software. Due to arranging single antenna elements linearly in 1×4 MIMO configuration and introducing a DGS at bottom surface of the individual antenna elements, the radiating co-polarized (co-pol) patterns mainly focus on the broadside direction in the YZ-plane which makes a great enhancement in gain over mmWave band. In YZ-plane, the co-pol and cross-pol difference is > 25 dB at 27 and 38 GHz resonances as depicted in Fig. 12. It is also apparent that in the XZ-plane, the MIMO antenna maintains nearly omnidirectional co-polarized patterns. Furthermore, the co- and cross-pol difference is minimized due to large CPW ground plane on top surface of the mmWave MIMO antenna.

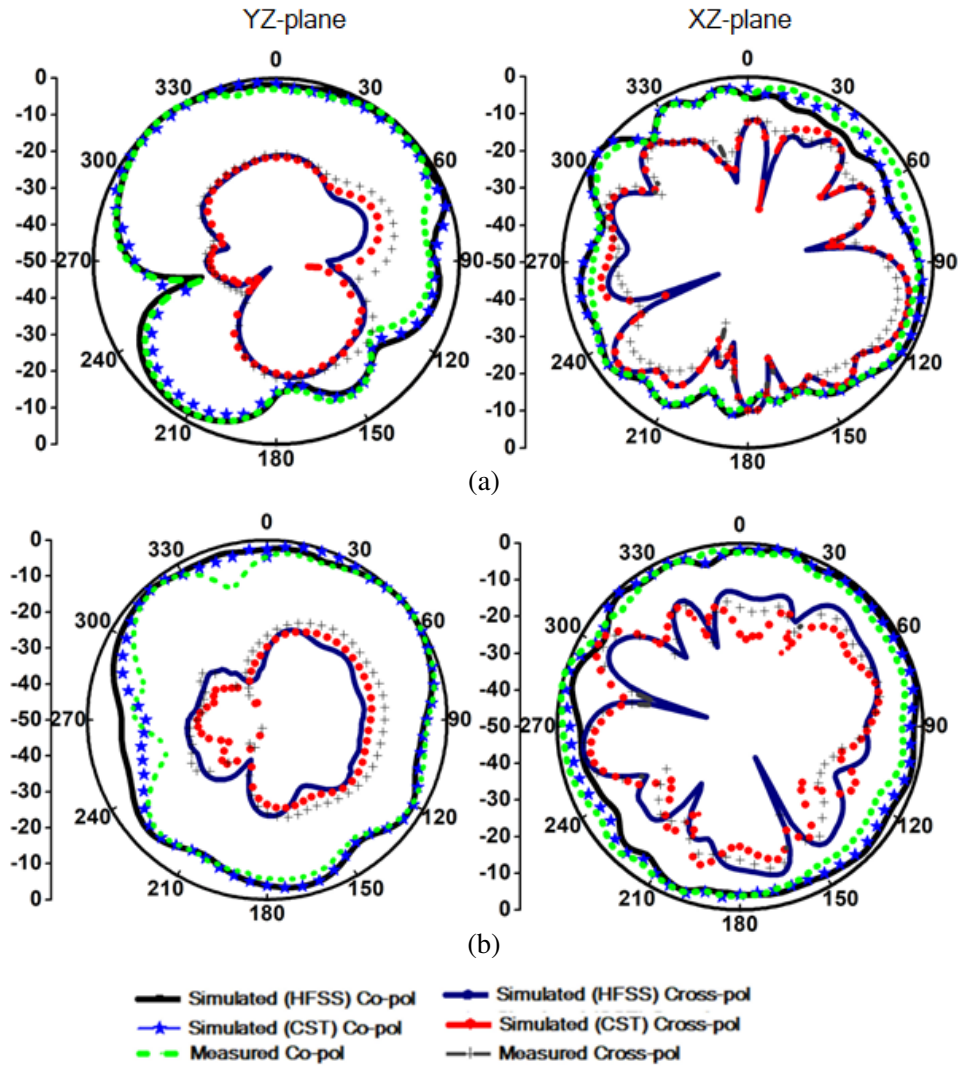

Figure 12. Comparison of far-field radiation patterns of proposed DGS based mmWave MIMO antenna array, (a) at 27 GHz and (b) at 38 GHz.

5.2. Diversity Performance Analysis of DGS Based mmWave MIMO Antenna Array

The diversity performance of the proposed 4-element DGS loaded mmWave MIMO antenna array is evaluated through ECC, diversity gain (DG), CCL, and total active reflection coefficient (TARC) in this section.

The ECC defines the correlation among antenna elements for diversity performance, and it can be computed from S-parameters through Eq. (1) [33].

$$\rho_{eij} = |\rho_{eij}|^2 = \left| \frac{S_{ii}S_{ij}^* + S_{ji}S_{jj}^*}{|(1 - S_{ii} - S_{ji})(1 - S_{jj} - S_{ij})|^{1/2}\, \eta_{rad_i}\eta_{rad_j}} \right|^2 \tag{1}$$

where ρ_{eij} is the ECC; S_{ij}/S_{ji} represent the coupling parameter between i/j and j/i elements; η_{radi} and η_{radj} are the radiation efficiency factors for i and j elements, respectively. The appropriate value of ECC should be < 0.5 for good diversity performance. The DG (dB) can be calculated from ECC through Eq. (2) [33].

$$DG = 10 * \sqrt{1 - |\rho_{eij}|^2} \tag{2}$$

For good diversity performance, the accepted value of DG should be around 10 dB in the band of interest. The ECC, DG, CCL, and TARC have been analysed when port 1 is excited, and remaining ports (ports 2, 3 and 4) are matched through 50 Ω load. The simulated ECC and DG by using HFSS and CST MWS are depicted in Fig. 13. It is found from S-parameters that ECC < 0.0014 and DG almost 10 dB (> 9.999994 dB). Similarly, it is also observed from far-field that ECC < 0.0016 and DG > 9.999992 dB which ensure the good diversity performance at mmWave band.

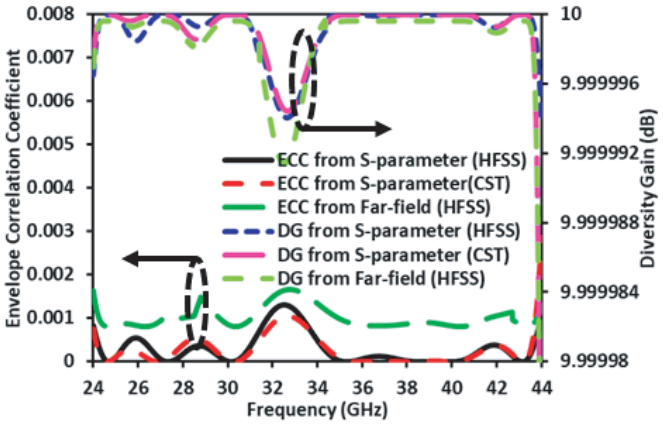

Figure 13. ECC and DG plots of the proposed DGS based mmWave MIMO antenna array.

CCL is another key parameter that provides channel capacity loss during the correlation effect of MIMO system and the accepted value of CCL < 0.5 bits/sec/Hz for good diversity [33]. Correspondingly, TARC is an important characteristic of a MIMO system to achieve effective impedance bandwidth. It is the ratio of the square root of the total reflected power to the total incident power [33] and the accepted value of TARC < 0 dB. Figs. 14(a) and (b) show the CCL and TARC of the proposed DGS based 4-element mm-Wave MIMO antenna, respectively. The CCL < 0.29 bits/sec/Hz and TARC < -10 dB are attained by using HFSS and CST MWS over mmWave band which ensure good diversity performance.

5.3. Comparison with Published Works

In Table 6, the performance comparison in terms of antenna size, number of elements, antenna type, -10 dB bandwidth, peak gain, isolation, and ECC of the proposed GCPW-fed DGS loaded 4-element mmWave MIMO antenna with the cited mmWave works is summarized. The DR based 2-element

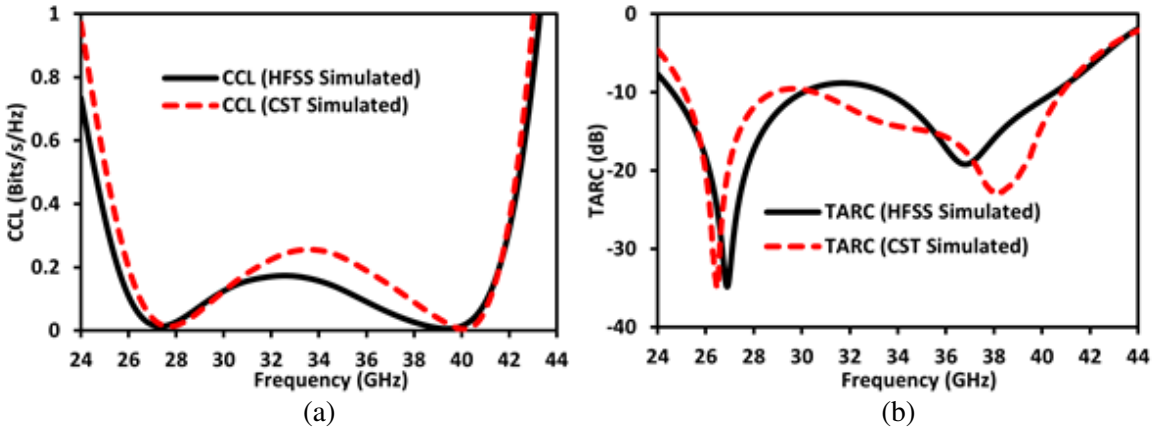

Figure 14. (a) CCL and (b) TARC plots of the proposed DGS based mmWave MIMO antenna array.

MIMO antenna [13] and helix 2-element MIMO antenna [24] have very small bandwidth about 5.88% and 13.88%, low peak gain about 7.0 dBi and 5.83 dBi, and low ECC about 0.002 and 0.005, respectively. The DGS and metamaterial loaded 4-port mmWave MIMO antennas [18, 28–31] have the large antenna size, complex structures, small −10 dB bandwidths, high mutual coupling, and low peak gains, but the antenna [30, 31] has good isolation and ECC. The tree shaped monopole MIMO antenna [25] has 53.96% bandwidth but large antenna size and high mutual coupling. It is also observed that the proposed DGS based MIMO antenna provides the highest fractional bandwidth of about 49.62% in contrast to other

Table 6. Comparative analysis of the proposed GCPW-fed 4-element mmWave MIMO antenna array with cited 2-/4-element mmWave MIMO works.

S. No.	Antenna Size (λ^3) (at lowest frequency)	No. of elements	Antenna Type	−10 dB Bandwidth (GHz, $f_{\text{span\|GHz}}$, %)	Isolation (dB)	Gain (dBi)	ECC
[13]	2.08 × 4.75 × 0.307	2	DR Based MIMO Antenna	29.7–31.5, 1.8, 5.88	> 25	7.0	0.002
[18]	1.00 × 4.25 × 0.067	4	DGS Based MIMO Antenna	25.1–37.5, 12.4, 39.61	> 22	10.6	0.005
[24]	1.31 × 2.19 × 0.018	2	Helix MIMO Antenna	26.25–30.14, 3.98, 13.88	> 30	5.83	0.005
[25]	6.13 × 6.13 × 0.120	4	Tree Shaped Monopole MIMO Antenna	23–40, 17, 53.96	> 20	12	0.0014
[28]	2.69 × 4.16 × 0.022	4	Metamaterial Loaded MIMO Antenna	26.0–31.0, 5.0, 17.54	> 21	10.0	0.0015
[29]	2.55 × 2.98 × 0.065	4	DGS Based MIMO Antenna	25.5–29.6, 4.1, 14.88	> 17	8.3	0.01
[30]	2.64 × 2.64 × 0.139	4	DGS Based MIMO Antenna	26.4–29.75, 3.35, 11.93	> 30	7.1	0.0005
[31]	2.75 × 3.20 × 0.072	4	DGS Based MIMO Antenna	27.5–28.5, 1.0, 3.57	> 40	12	0.0003
This Work	**1.02 × 3.86 × 0.021**	**4**	**DGS Based MIMO Antenna**	**25.30–42, 16.70, 49.62**	> 24	**12.02**	**0.0014**

DGS based MIMO antennas [18, 29–31]. Based on the study from Table 6, the proposed DGS loaded 4-element mmWave MIMO antenna array in comparison to cited state-of-art quad-element mmWave MIMO antenna designs has planar structure, smaller antenna size of $1.02\lambda \times 3.86\lambda \times 0.021\lambda$, and wider bandwidth about 16.70 GHz (49.62%) except [25], isolation > 24 dB, high peak gain about 12.02 dBi, and high ECC about 0.0014. With these features of small size, wider bandwidth, and excellent diversity performance (CCL < 0.29 bits/sec/Hz and TARC < -10 dB), the proposed 4-element mmWave MIMO antenna array with DGS is a favourable candidate for 5G mmWave communication especially 5G enabled portable devices and base stations operating at n257 band (26.5–29.5 GHz), n260 band (37.0–40.0 GHz), n261 band (27.5–28.35 GHz), and other frequency range 2 (FR2) based future 5G new radio (NR) bands.

6. CONCLUSION

In this article, a low-profile GCPW-fed DGS based four-element MIMO antenna array is successfully designed, fabricated, and tested. An efficient single-element antenna design offering wide bandwidth and asymmetrical inverted T-shaped slots is embedded in partial ground plane as DGS in the GCPW-fed deformed pentagonal patch antenna. The proposed DGS based 4-element MIMO antenna array is realized by arranging the 4 identical antenna elements linearly in a 1×4 manner with a distinct gap without any decoupling structure. The MIMO antenna array with DGS yields a -10 dB impedance bandwidth of 16.70 GHz (25.30–42.00 GHz), isolation > 24 dB, and peak gain about 12.02 dBi over the entire mmWave band. Performance of the proposed DGS based 4-element mmWave MIMO antenna array has been further explored for MIMO systems and exhibits ECC < 0.0014, DG ~ 10 DB, CCL < 0.3 bits/sec/Hz, and TARC < -10 dB. In order to provide many benefits including planar geometry, compact size, wide bandwidth, high isolation without any decoupling structure, high gain without additional reflecting surfaces, and low ECC over mmWave frequency range, the proposed DGS based MIMO antenna array is a promising candidate for 5G mmWave communication especially 5G enabled portable devices and base stations operating at n257 band (26.5–29.5 GHz), n260 band (37.0–40.0 GHz), n261 band (27.5–28.35 GHz), and other frequency range 2 (FR2) based future 5G new radio (NR) bands.

REFERENCES

1. Thompson, J., X. Ge, H. C. Wu, R. Irmer, H. Jiang, G. Fettweis, and S. Alamouti, "5G wireless communication systems: Prospects and challenges," *IEEE Commun. Mag.*, Vol. 52, No. 2, 62–64, 2014.
2. Wang, C. X., F. Haider, X. Gao, X. H. You, Y. Yang, D. Yuan, H. M. Aggoune, H. Haas, S. Fletcher, and E. Hepsaydir, "Cellular architecture and key technologies for 5G wireless communication networks," *IEEE Commun. Mag.*, Vol. 52, No. 2, 122–130, 2014.
3. Rangan, S., T. S. Rappaport, and E. Erkip, "Millimeter-wave cellular wireless networks: Potentials and challenges," *Proc. IEEE*, Vol. 102, No. 3, 366–385, 2014.
4. Desai, A., T. Upadhyaya, J. Patel, R. Patel, and M. Palandoken, "Flexible CPW fed transparent antenna for WLAN and sub-6 GHz 5G applications," *Microw. Opt. Technol. Lett.*, Vol. 62, No. 5, 2090–2103, 2020.
5. Li, Q. L., S. W. Cheung, D. Wu, and T. I. Yuk, "Optically transparent dual-band MIMO antenna using micro-metal mesh conductive film for WLAN system," *IEEE Antennas Wirel. Propag. Lett.*, Vol. 16, 920–923, 2016.
6. Hussain, R., A. T. Alreshaid, S. K. Podilchak, and M. S. Sharawi, "Compact 4G MIMO antenna integrated with a 5G array for current and future mobile handsets," *IET Microw, Antennas Propag.*, Vol. 11, No. 2, 271–279, 2017.
7. Prabhu, P. and S. Malarvizhi, "Novel double-side EBG based mutual coupling reduction for compact quad port UWB MIMO antenna," *AEU — Int. J Electron. Commun.*, Vol. 109, 146–156, 2019.
8. Akbari, M., H. A. Ghalyon, M. Farahani, A. R. Sebak, and T. A. Denidni, "Spatially decoupling of CP antennas based on FSS for 30-GHz MIMO systems," *IEEE Access*, Vol. 5, 6527–6537, 2017.

9. Malaisamy, K., M. Santhi, and S. Robinson, "Design and analysis of 4×4 MIMO antenna with DGS for WLAN applications," *Int. J. Microw. Wirel. Technol.*, Vol. 13, No. 9, 979–985, 2021.
10. Dharmarajan, A., P. Kumar, and T. J. O. Afullo, "A high gain UWB human face shaped MIMO microstrip printed antenna with high isolation," *Multimed Tools Appl.*, Vol. 81, 34849–34862, 2022.
11. Kumar, A., A. Kumar, and A. Kumar, "Gain enhancement of a wideband rectangular ring monopole millimeter-wave antenna using artificial magnetic conductor surface," *Int. J. RF Microw. Comput. Aided Eng.*, Vol. 32, No. 10, e23319, 2022.
12. Ibrahim, A. A. and W. A. Ali, "High gain, wideband and low mutual coupling AMC-based millimeter wave MIMO antenna for 5G NR networks," *AEU — Int. J. Electron. Commun.*, Vol. 142, 153990, 2021.
13. Sharawi, M. S., S. K. Podilchak, M. S. Hussain, and Y. M. M. Antar, "Dielectric resonator based MIMO antenna system enabling millimetre-wave mobile devices," *IET Microw., Antennas Propag.*, Vol. 11, 287–293, 2017.
14. Thakur, V., N. Jaglan, and S. D. Gupta, "Side edge printed eight-element compact MIMO antenna array for 5G smartphone applications," *Journal of Electromagnetic Waves and Applications*, Vol. 36, No. 12, 1685–1701, 2022.
15. Jaglan, N., S. D. Gupta, B. K. Kanaujia, and M. S. Sharawi, "10 element sub-6-GHz multi-band double-T based MIMO antenna system for 5G smartphones," *IEEE Access*, Vol. 9, 118662–118672, 2021.
16. Kiani, S. H., A. Altaf, M. R. Anjum, S. Afridi, Z. A. Arain, S. Anwar, S. Khan, M. Alibakhshikenari, A. Lalbakhsh, M. A. Khan, et al., "MIMO antenna system for modern 5G handheld devices with healthcare and high rate delivery," *Sensors*, Vol. 21, 7415, 2021.
17. Ali, S. A., M. Wajid, M. Usman, and M. S. Alam, "A high-order EMSIW MIMO antenna for space-constrained 5G smartphone," *Sensors*, Vol. 21, 8350, 2021.
18. Jilani, S. F. and A. Alomainy, "Millimeter-wave T-shaped MIMO antenna with defected ground structures for 5G cellular networks," *IET Microw., Antennas Propag.*, Vol. 12, No. 5, 672–677, 2018.
19. Gupta, A. and V. Kumar, "DGS-based wideband MIMO antenna for on-off body communication with port isolation enhancement operating at 2.45 GHz industrial scientific and medical band," *Journal of Electromagnetic Waves and Applications*, Vol. 35, No. 7, 888–901, 2021.
20. Madhav, B. T. P., Y. Usha Devi, and T. Anil Kumar, "Defected ground structured compact MIMO antenna with low mutual coupling for automotive communications," *Microw. Opt. Technol. Lett.*, Vol. 61, No. 3, 794–800, 2019.
21. Xing, H., X. Wang, Z. Gao, X. An, H. X. Zheng, M. Wang, and E. Li, "Efficient isolation of an MIMO antenna using defected ground structure," *Electronics*, Vol. 9, No. 8, 1265, 2020.
22. Venkateswara Rao, M., B. T. P. Madhav, J. Krishna, Y. Usha Devi, T. Anil Kumar, and B. Prudhvi Nadh, "CSRR-loaded T-shaped MIMO antenna for 5G cellular networks and vehicular communications," *Int. J. RF Microw. Comput. Aided Eng.*, Vol. 29, No. 8, 21799, 2019.
23. Qiu, H., H. Liu, X. Jia, Z. Y. Jiang, Y. H. Liu, J. Xu, T. Lu, M. Shao, T. L. Ren, and K. J. Chen, "Compact, flexible, and transparent antennas based on embedded metallic mesh for wearable devices in 5G wireless network," *IEEE Trans. Antennas Propag.*, Vol. 69, No. 4, 1864–1873, 2020.
24. Zahra, H., W. A. Awan, W. A. E. Ali, N. Hussain, S. M. Abbas, and S. Mukhopadhyay, "A 28 GHz broadband helical inspired end-fire antenna and its MIMO configuration for 5G pattern diversity applications," *Electronics*, Vol. 10, No. 4, 405, 2021.
25. Sehrai, D. A., M. Abdullah, A. Altaf, S. H. Kiani, F. Muhammad, M. Tufail, M. Irfan, A. Glocks, and S. Rahman, "A novel high gain wideband MIMO antenna for 5G millimeter wave applications," *Electronics*, Vol. 9, No. 6, 1031, 2020.
26. Gupta, S., Z. Briqech, A. R. Sebak, and T. A. Denidni, "Mutual-coupling reduction using metasurface corrugations for 28 GHz MIMO applications," *IEEE Antennas Wirel. Propag. Lett.*, Vol. 16, 2763–2766, 2017.

27. Aghoutane, B., S. Das, M. E. Ghzaoui, B. T. P. Madhav, and H. El Faylali, "A novel dual band high gain 4-port millimeter wave MIMO antenna array for 28/37 GHz 5G applications," *AEU — Int. J. Electron. Commun.*, Vol. 145, 154071, 2022.
28. Wani, Z., M. P. Abegaonkar, and S. K. Koul, "A 28-GHz antenna for 5G MIMO applications," *Progress In Electromagnetics Research Letters*, Vol. 78, 73–79, 2018.
29. Khalid, M., S. I. Naqvi, N. Hussain, M. U. Rahman, and Y. Amin, "4-port MIMO antenna with defected ground structure for 5G millimeter wave applications," *Electronics*, Vol. 9, No. 1, 71, 2020.
30. Hussain, M., E. Mousa Ali, S. M. R. Jarchavi, A. Zaidi, A. I. Najam, A. A. Alotaibi, A. Althobaiti, and S. S. M. Ghoneim, "Design and characterization of compact broadband antenna and its MIMO configuration for 28 GHz 5G applications," *Electronics*, Vol. 11, No. 4, 523, 2022.
31. Bilal, M., S. I. Naqvi, N. Hussain, Y. Amin, and N. Kim, "High-isolation MIMO antenna for 5G millimeter-wave communication systems," *Electronics*, Vol. 11, 962, 2022.
32. Ullah, S., W. H. Yeo, H. Kim, and H. Yoo, "Development of 60-GHz millimeter wave, electromagnetic bandgap ground planes for multiple-input multiple-output antenna applications," *Sci. Rep.*, Vol. 10, 8541, 2020.
33. Kumar, A., A. Kumar, P. J. Soh, and A. Kumar, "Design consideration, challenges and measurement aspects of 5G mm-Wave antennas: A review," *Progress In Electromagnetics Research B*, Vol. 96, 39–66, 2022.